Proceedings of ASME Turbo Expo 2011
GT2011
June 6-10, 2011, Vancouver, British Columbia, Canada

GT2011-46203

Determination of crack initiation on L-1 LP steam turbine blades, Part 1: Measurements on rotor train, material specimens and blades

Zdenek Kubin, Vaclav Cerny, Pavel Panek, Tomas Misek, Jan Hlous, Lubos Prchlik
SKODA Power s.r.o.
Research & Development
Tylova 1/57, Plzen, Czech Republic, 30100
Czech Republic
Email: zdenek.kubin@doosanskoda.com

Abstract

After 10 years of operation of a steam turbine with large output power there was an accident during the turbine run-up. One of rotating blade fell off. All 6 LP rotors (two machines) were checked and many cracks on the L-1 blades were found. Due to economic reasons, blades with an identical geometry were manufactured quickly and a new material was used. A better material was chosen in terms of yield limit. The egalization of rotor grooves was performed because of manufacturing accuracy. Tip-timing measurement was installed on two L-1 stages to monitor and protect the blades.

After one year of smooth operation new inspections were made. Surprisingly, it was found that the blades made of the new material had comparatively more cracks than the original blades. A new investigation has been started. This article describes measurements including rotor torsional excitation, blade tip-timing measurements, modal analysis and material tests. A computational analysis is presented in Part 2. Application of both approaches revealed what hypotheses should be rejected and, on the other hand, which of them should be analyzed in a deeper way. Consequently, the unstalled flutter has been identified as the most probable cause of blade cracks.

INTRODUCTION

Two years ago cracks on L-1 free-standing blades were detected, when one blade failed and damaged the last two stages in LP part of a steam turbine. Non-destructive examination (faced array) indicated that approximately one third of the blades had cracks.

A laboratory evaluation of the cracking indicated the failure mechanism to be high cycle fatigue. On fracture surfaces there was found striation corresponding to the number of turbine run-ups. The cracks were situated in the first radius of the fir-tree root, where the maximum stress from first and second bending mode is concentrated. The initiation of the cracking observed along the radius of the top attachment hook is likely due to stress corrosion cracking. Several surface conditions were observed within the hooks that could have contributed to crack initiation, which include machining grooves, fretting, scratches and possible pitting.

The damaged blades were replaced by blades from a new material, but the design was maintained. During the repairs several tests were performed.

One of theories about the cause of the cracks was the resonant vibration. First, the natural frequencies of blades were recalculated and measured inside a balancing vacuum tunnel using a telemetry system. As it was expected the natural frequencies were far away from possible rotor excitation frequencies (all multiples of 50 Hz up to 400 Hz). Mistuning phenomena were in scope of view because cracked blades were aggregated to several groups.

Before the run-up a tip-timing measurement was installed into the LP part of the turbine to collect the vibration information of the blades. Several papers describe blade failure due to rotor torsional vibration [1]. There was strain gage telemetry system installed between last LP part and generator to obtain the rotor torsional vibration. In addition, generator data were studied and electromagnetic moment, which goes hand in hand with torsion of generator, was computed from the measured data (voltage, current).

All these tests were performed throughout the whole year, when the machine worked with new and original blade stages. After one year of operation the machine was stopped and new face array tests were applied to all blades. A surprising finding was made that there were cracks on the newly installed blades from the new material (T552) but no cracks on one stage with blades made only of the original material (AK1TD). The blades with cracks were sharply separated into groups. That implies new direction in investigation contains the damping and looking for instability especially for flutter.

TORSION EXCITATION

A torsional excitation of the rotor train together with torsional vibrations of the train have also been analyzed in order to confirm or reject these phenomena as the cause of low pressure blade cracks. The torsional excitation of the train, which has been taken into account, is produced by the generator through its electromagnetic torque that torsionally strains the train. Measurement positions of the torsional vibrations of the train have been put onto the front part of the high pressure rotor and an end part of the generator exciter. A group of time series of the electromagnetic torque and the torsional vibrations of the train has been measured and subsequently analyzed by an algorithm of *Short Time Fourier Transform* implemented in Matlab. The sampling frequency of the series was 3000 Hz and they contained several different events that have been analyzed step by step. The following events have been studied:

- nominal operation
- suppressor connection
- line short-circuit
- line forced outage
- generator and grid disconnection

For instance, results of a spectral analysis of the line short-circuit event are given at Fig. 1.

While going through all results of the spectral analysis of the time series that included the events mentioned above, it has been found out that neither the torsional excitation of the rotor train nor torsional vibrations of the train are the cause of low pressure blade cracks. There are two main reasons for making this conclusion. The first one says that there is not any frequency in the time series of the torsional vibrations of the train around the frequency 170Hz that could work up the first bending mode of the blades whose natural frequency is just the value 170Hz while the blades increasingly vibrate along this bending mode at

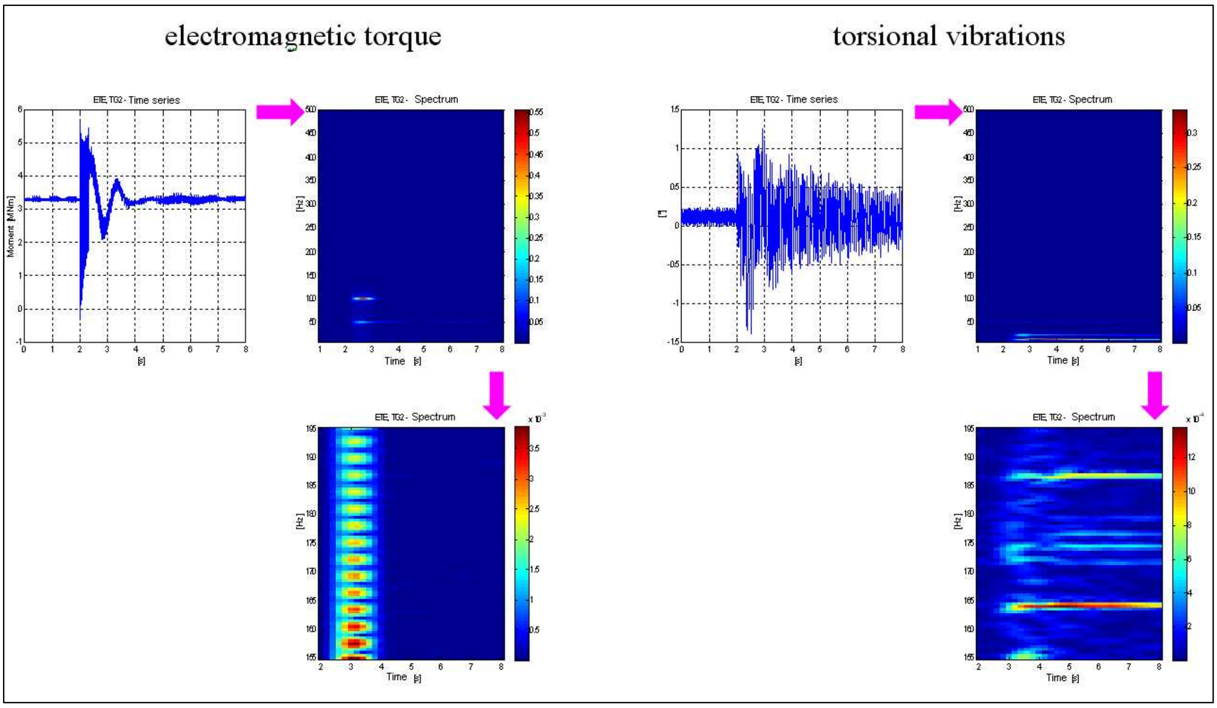

Fig. 1 - Amplitude spectra of time series of electromagnetic torque and torsional vibrations

operation (see above). At second, there are frequencies involved in the time series of the electromagnetic torque around the frequency 170Hz (e.g. see the Fig. 1). Nevertheless, their amplitudes are too small in order to work up the first bending mode of the blades. The second reason has also been proved computationally based on FEM.

MISTUNING

Each blade made by Skoda goes through the quality control. The natural frequency, weight and static moment are measured blade by blade. This information was used to calculate correlation between blades with/without crack, their frequency and static moment. There was no correlation found between those parameters. Figure 2 shows frequency and static moment deviation on one of 12 stages. It is clear that there is no dependence of cracks on frequency or static moment.

Next step was to create the model of a mistuned bladed disk. This model was excited by electromagnetic torque moment measured on the generator. Only 0 ND was excited and maximum stress did not reach the critical value. During operation the vibration amplitude can be amplified by a close resonant frequency, but the nearest torsional resonant frequency was calculated far away from the blade resonant frequency 170 Hz.

TIP-TIMING

As the most important measurement the Blade Tip-Timing (BTT) was installed to observe blade vibration on-line. BTT was installed on two L-1 stages and on one L-0 stage. The last L-0 stage ran smoothly without vibration and it will not be considered further in this article.

When the machine ran up to 3000 RPM and power reached 1000MW, the BTT gave us results that showed that the L-1 blades vibrate dominantly according to the first bending mode at 170 Hz. Using the ANSYS software modal analysis was performed and the results were used for BTT calibration. The blades' bending mode direction is 61° from rotor axial direction. The maximum stress is located at the radius of the top blade hook (see Fig. 5).

There is centre tip deviation Y´ = 0.94 mm and it corresponds to alternate bending radial stress σ_a (see Fig. 5).

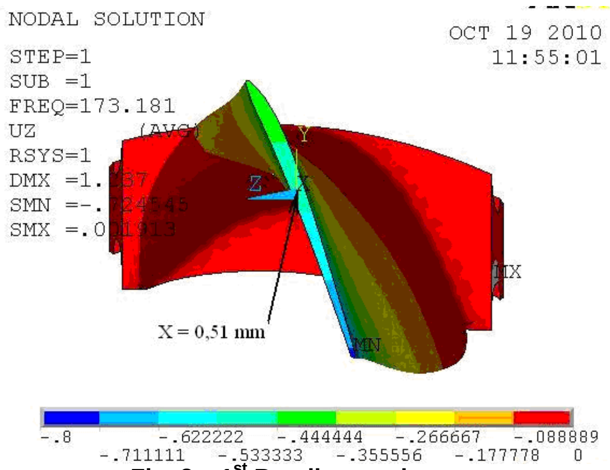

Fig. 3 – 1st Bending mode

Blades L-1 were made of T552 alloy. The Haigh diagram is depicted in Fig. 4. In the diagram there are fatigue limit curves of an ideal body and of a measured sample which corresponds to the shape of the real fir-tree hook. Tests were performed with tension / pressure bias superimposed to σ_s and all values correspond to the nominal tension in the hook. The hook of the blade at 3000 RPM is loaded by tensile stress σ_s = 250 MPa. For this tension, the value of allowable stress $\sigma_{a\text{-}allow}$ (safety factor of 2, includes corrosive environment) was plotted into the Haigh diagram.

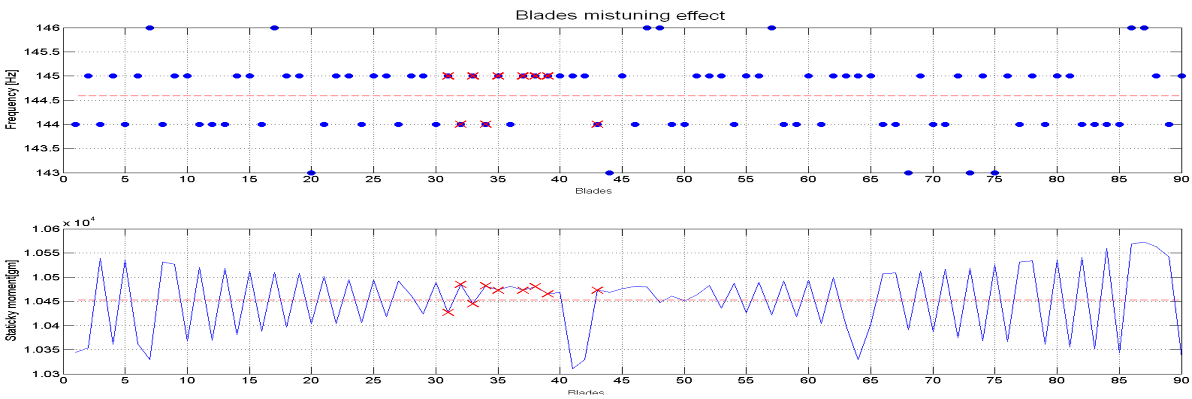

Fig. 2 - Frequency and static moment deviation along the blisk

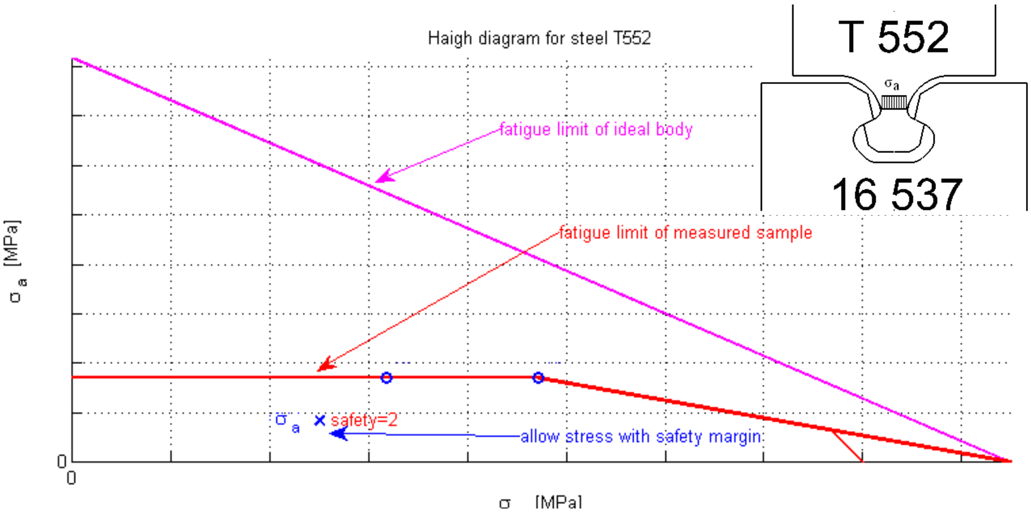

Fig. 4 - Haigh diagram of T552 and picture of the measured sample

Displacement of the tip profile in the tip-timing method is calculated from the time differences Δt using the formula

$$Yc = 2 \cdot \pi \cdot f \cdot Rs \cdot \Delta t \,,$$

where f is rotation frequency (50Hz) and Rs is the radius of the rotating blade tip. Blade vibrates in the V direction (see Fig.6), at an angle β = 61° to the axial direction of the rotor. The blade is shown in Fig.6 and is approximated by abscissa with an angle α = 20° to the rotor tangential direction. The figure shows that the movement can be decomposed into the directions x (X), y (Y '). When moving in the direction x (A → A '), the blade moves relative to the sensor (s). When moving in the direction y (A '→ A"), the blade also moves towards the sensor (Y'). Total vibration of the blade (A → A") measured by sensor is Y_C.

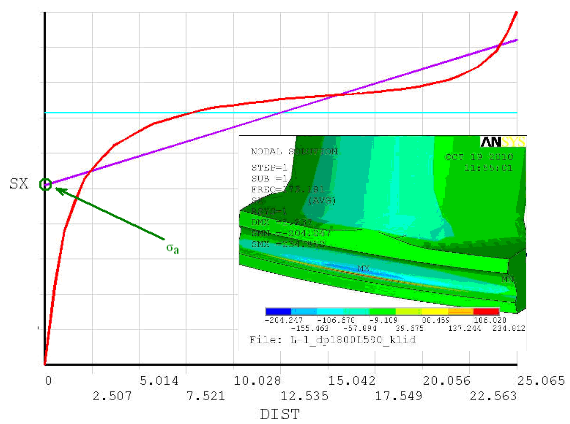

Fig. 5 - The stress along the hook corresponding to deflection in Fig. 3

The geometric relations and real computed data yield these equations:

$$Yc = Y + Y' \,,$$

$$X = \frac{Y'}{tg(\beta)} = 0.55 \cdot Y' \,,$$

$$Y = \frac{X}{tg(\alpha)} = 2.75 \cdot X \,,$$

$$Yc = (2.75 \cdot 0.55 + 1) \cdot Y' = 2.51 \cdot Y' \,.$$

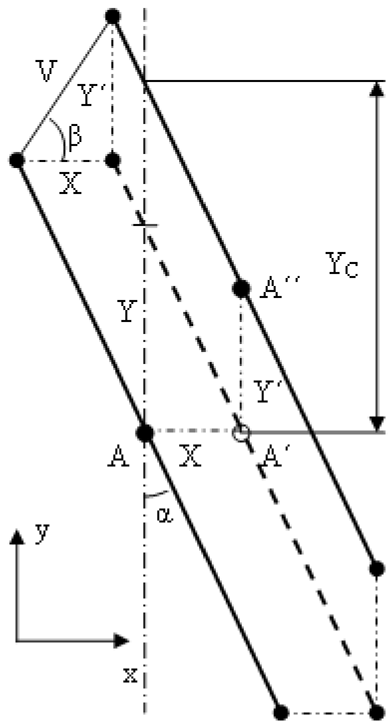

Fig. 6 - Geometric relations and BTT calibration

The maximum acceptable displacement of blade tip $Y'_D = 0.94$ mm corresponds to the maximum blade tip displacement measured by tip-timing Y_C:

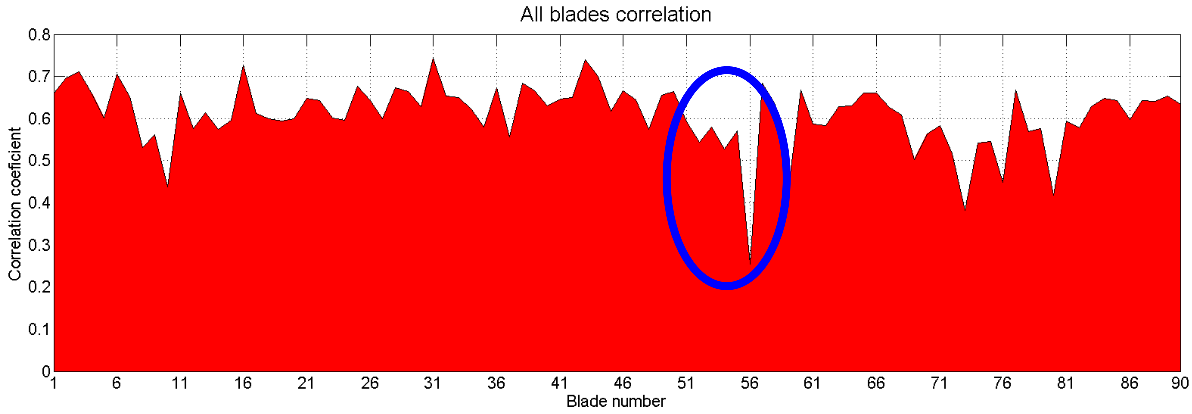

Fig. 7 - Blade vibration and counterpressure correlation

$$Yc = 2.51 \cdot 0.94 = 2.36\ mm\,.$$

$$\Delta t = \frac{Yc}{2 \cdot \pi \cdot f \cdot Rs} = \frac{2.36}{2 \cdot \pi \cdot 50 \cdot 1500} = 5.01\ \mu s$$

$$\Delta t(RMS) = \frac{\Delta t}{\sqrt{2}} = 3.54\ \mu s\,.$$

.

The frequencies and amplitudes were monitored during the year. It was observed that the largest amplitudes occurred during start-up at 700MW power. After that the amplitude decreased slowly until the end of year (see Fig. 8).

The largest vibration was found at the blade number 56. Three neighboring blades also vibrated at high amplitude. After one year of operation, when the machine was stopped due to reactor refuelling, the face-array analysis was performed and these blades had a crack. The crack initiation was not accompanied with a change in the first natural frequency as expected. The frequencies were evaluated from the first and the last month of operation using Hilbert-Huang transformation [2]. This method had to be used because of non-stationary amplitude.

The correlation of BTT amplitude to counterpressure, vacuum and other operating parameters were calculated. The blades with crack had the lowest correlation coefficient in each particular correlation. This fact told us that we did not find any excitation forces and it could be some type of instability. The correlation coefficients were calculated as:

$$r_k = \frac{\sum_{t=1}^{N}(x_t - \bar{x}) \cdot (x_{t+k} - \bar{x})}{\sum_{t=1}^{N}(x_t - \bar{x})^2}$$

where x_k is a data value at time step t, k is the lag, and the overall mean is given by standard equation.

DAMPING AND MATERIAL PROPERTIES

New material had to be chosen instead of old one AK1-TD which is not available any more. T552 is a creep resisting, corrosion resistant hardened and tempered steel, with good toughness and good creep rupture strength. T671 is a creep resisting Cr-Ni-Mo-Cu martensitic precipitation hardenable steel with high strength and toughness.

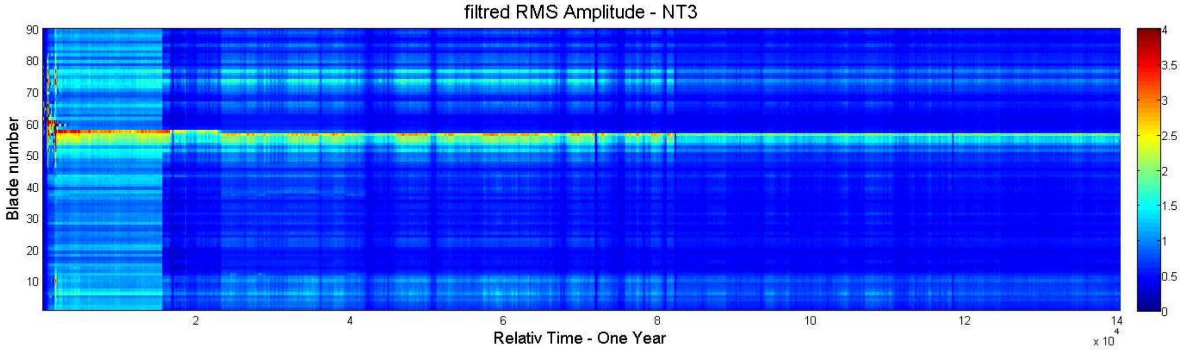

Fig. 8 - BTT vibration of all blades during one year

AK1-TD is a modified 12% Cr martensitic steel.

Mechanical properties of these alloys could be seen in Tab.1. It is apparent that steel T552 exceeds all mechanical characteristics of steel AK1-TD except for elongation, in case of which they are comparable.

Microstructure of alloys T552 and AK1-TD after heat treatment is sorbitic with fine grain size. Microstructure of alloy T671 after hardening is martensitic with dispersed particles of carbides and fine grain size. Maximal allowed amount of delta-ferrite is 1% for alloys T552 and T671 and 5% for alloy AK1-TD.

Table 1 - Mechanical properties of alloys T552, T671 and AK1-TD

		T552	T671	AK1-TD
Yield Strength R_e	MPa	min. 800	min.1030	min. 670
Ultimate Tensile Strength R_m	MPa	950 – 1070	1100 – 1250	840 – 1000
Elongation A_5	%	min. 14	min. 10	min. 15
Impact Energy KV	J	min. 55	min. 80	min. 25
Hardness HB		292 - 330	330 – 360	255 – 305

Other important feature which is not in standard tables is damping. Damping (ξ) is one of two factors determining the differential equation and system stability.

$$\ddot{y}(t) + 2 \cdot \xi \cdot \varpi \cdot \dot{y}(t) + \varpi^2 \cdot y(t) = 0$$

It is easy to see if the damping is positive the system is stable and negative damping cause instability. In real case, this damping ξ contains material, construction and aerodynamic damping. The material damping was measured on free standing blade and on material sample. The blade was suspended on thin steel string and excited by modal hammer. The damping was evaluated as

$$\xi = \frac{1}{2 \cdot \pi} \cdot \ln \frac{A_1}{A_2}$$

and parallel using LMS algorithm to fit local maximum of real filtered signal with the part of differential equation solution $x(t) = e^{-\xi \cdot \varpi \cdot t}$. The ultrasonic measurement was chosen as second method to find out material damping of material sample.

The construction damping can not be measured without material damping. This combination of damping was measured on blisk before the machine start (0 RPM) and during the run-ups using Tip-Timing (there are not enough steam on LP part during run-up, the main power goes through HP). Local Rational Fraction Polynomial method [6] was used to evaluate blisk damping and as a complementary method it was used frequency bend of 3db decrease. To obtain usable frequency responds curve, the electromagnetic excitation was used with slow sweep function.

$$\xi = \frac{\varpi_2 - \varpi_1}{2\Omega_n}$$

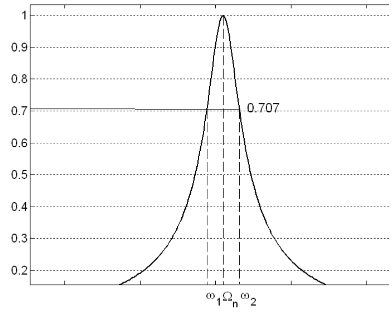

Fig. 9 - Frequency response function

All of methods which were used give us good significant results. From the accuracy and stability points of view, LMS fitting method provided the best results. It seems that material AK1-TD has bigger material damping than the other mentioned materials.

The damping measurement on blisk showed us big influence of blade – disk assembly (see Fig. 10). The blades in egalized groves (with more precision and lower wills) had lower damping because there was not additional friction in these grooves. The evaluation of blisk damping is little bit hard because of presence of Nodal Diameter (ND) and mistuning cause that several frequency peaks are really close. The best choice was inhibit or detune the rest of blades except the measured blade.

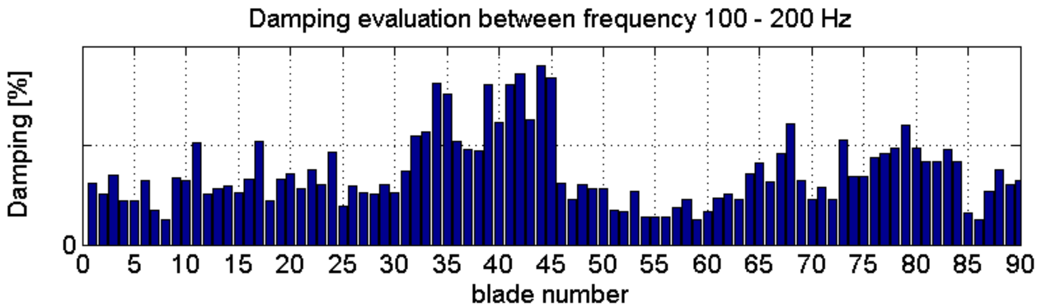

Fig. 10 - Damping measured at 0 RPM after blade assembly

FLUTTER

The aerodynamic instability known as flutter was investigated as another possible cause of the blade damage. Flutter is a state of self-excited oscillation of a lifting surface caused by the aerodynamic forces of the surrounding flow. For flutter to occur, the airfoil must move periodically (usually in one of its natural modes of oscillation), with the resulting oscillating pressure field of the surrounding fluid supplying energy into the airfoil. This energy corresponds to aerodynamic damping of the fluid-blade system; if this energy supply is positive, the aerodynamic damping is negative and vice versa. Negative aerodynamic damping indicates instability of the blade with respect to flutter if mechanical damping is neglected.

Flutter is a frequent concern in turbomachinery design, where flutter conditions may lead to high cycle fatigue and subsequent blade failure, in particular for thin and highly loaded blades. In steam turbines, the long low-pressure L-0 and L-1 stage buckets are potentially vulnerable to this type of self-excited oscillation.

CFD ANALYSIS

The freestanding, unshrouded low-pressure L-1 stage buckets of a large steam turbine were investigated for susceptibility to flutter by means of a three-dimensional, transient, RANS finite volume numerical analysis. The calculation was performed in the commercially available code ANSYS CFX 12.1 [3] using the methodology described by Mathias et al. [4]. The computational domain spanned over one half of the bladed disc assembly (180 degrees, 45 blade passages); this setting allowed computing all cases for which the nodal diameter *n* is an even number. A coarse mesh of approximately 20,000 nodes per passage was used. The mesh around each blade moved periodically according to the first bending mode shape as determined by modal analysis of the blade. The deformation was prescribed for all blades with an inter-blade phase angle defined by the nodal diameter. The nodal diameter and the inter-blade phase angle varied in the individual calculations. Fourteen runs were performed with nodal diameter set to -44, -32, -30, -28, -24, -20, -16, -12, -8, 0, +10, +16, +30 and +44. An example of the blade displacements at one point in time is shown in Fig. 11.

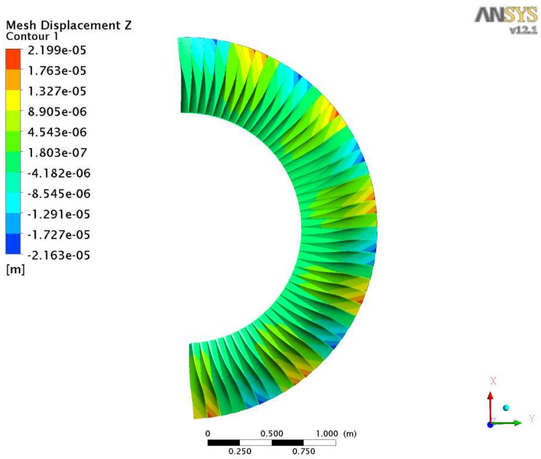

Fig. 11 - The modeled blades with mesh displacement in the axial (Z) direction at one point in time, nodal diameter n = -12

The boundary conditions of inlet total pressure, total temperature and velocity angle and exit static pressure represented the blade row operating at full load. With pressure ratio approximately 0.35, the mass flow rate through the blade row was 165 $kg.s^{-1}$.

Based on the time-dependent pressure and displacement data obtained from the calculation for each node on the blade surface, the work W transferred from the flow to the blade per one cycle of the blade motion was determined as

$$W = \sum_{steps} \sum_{faces} p\vec{A} \cdot \vec{x},$$

where p is the pressure on a face on the blade surface, $\vec{A}$ is the area normal vector of the face, $\vec{x}$ is the relative displacement vector in one time step and the summation takes place over all faces and all twenty-four time steps of a blade motion cycle.

This work was evaluated for each of the 45 blades and over six full blade motion cycles. The results were processed to obtain the average value from all blades and cycles in consideration together with the respective standard deviation. The logarithmic decrement δ, which represents the stability of the blade-fluid system in the absence of mechanical damping, was calculated as

$$\delta = -\frac{W}{2E},$$

where E is the maximum kinetic energy of the mode shape.

The results of the analysis are summarized in Fig. 12. The dependence of logarithmic decrement on nodal diameter indicates that the system is close to stability limit over a range of negative nodal diameters approximately from $n = -30$ to $n = -20$. However, the average aerodynamic damping remains positive for all nodal diameters examined. A more detailed CFD analysis including a calculation with a refined grid is necessary to confirm the instability.

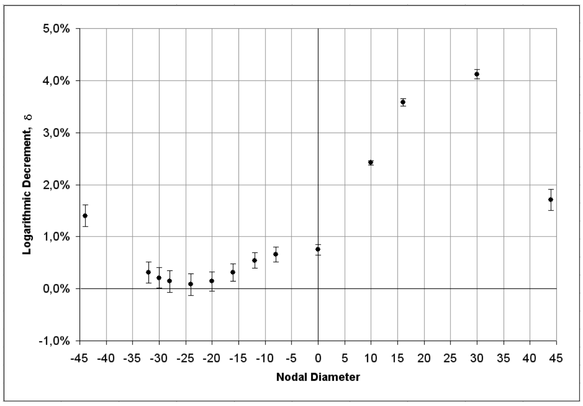

Fig. 12 - Logarithmic decrement plotted against the nodal diameter. The error bars correspond to one standard deviation of the data in each direction

CONCLUSION

At first, while going through all results of the spectral analysis of the time series of torsion that have included the specified events, it has been found out that neither the torsional excitation of the rotor train nor torsional vibrations of the train are a cause of low pressure blade cracks.

At second, the mistuning effect has also been rejected because cracks have been found on blades having different values of the first bending mode natural frequencies.

Finally, the cause of the blade cracks seems to be the unstalled flutter, which is typical for a high flow rate in the area of low pressure parts of steam turbines. The possibility of this type of flutter has been proved computationally indicated by a CFD analysis and its presence has been confirmed by the BTT measurement as well. It has also been confirmed by the BTT measurement that cracked blades are gathered to groups. The largest vibration amplitudes of the blades have been observed along fast output power changes. Vibration amplitudes of the blades can be described by the Gaussian probability distribution with a pretty high significance level (identified in virtue of the Lilliefors goodness of fit test). This means that they have a character of random variable, which implies that an excitation force cannot have any form of periodic wave. The conclusion is that the system of the bladed disc is found on stability margin due to aero-dynamical forces which cause the system being unstable (negative damping). This phenomenon is known as the unstalled flutter.

REFERENCES

[1] Rosario, Darryl A. "L-0 blade failure investigation at south texas project". 8th EPRI Turbine-Generator Conference. 2003.

[2] Norden E. Huang, Zheng Shen, Steven R. Long, Manli C. Wu, Hsing H. Shih, Quanan Zheng, Nai-Chyuan Yen, Chi Chao Tung and Henry H. Liu. "The empirical mode decomposition and the Hilbert spectrum for nonlinear and non-stationary time series analysis". Proc. R. Soc. Lond. A (1998) 454, 903-995

[3] ANSYS CFX 12.1, user manual

[4] Mathias, S., Woods, I., and Elder, R., "Integrated fluid structure interaction methodology for blade flutter analysis", Proceedings of the 12th International Symposium on Unsteady Aerodynamics, Aeroacoustics & Aeroelasticity of Turbomachines, London, UK, 2009.

[5] Richardson, M. H. & Formenti, D. L. "Global Curve Fitting of Frequency Response Measurements using the Rational Fraction Polynomial Method", Proceedings of the 3rd International Modal Analysis Conference, Orlando, Florida, January 28-31, 1985.

[6] Mark H. Richardson, "Global frequency & damping estimates from frequency response measurements", Presented at 4RD IMAC Conference, Los Angeles, CA, 1986

[7] Panovsky, J. and Kielb, R. E., "A Design Method to Prevent Low Pressure Turbine Blade Flutter," ASME Paper 98-GT-575, 1998

[8] Kielb, R., Barter, J., Chernysheva, O., Fransson, T.,"Flutter of Low-Pressure Turbine Blades with Cyclic Symmetric Modes – A Preliminary Design Method" ASME Paper GT2003-38694, 2003